

- MASSE, R. & GRENIER, J. (1971). *Bull. Soc. Fr. Mineral. Cristallogr.* **94**, 437–442.
- ROGERS, D. (1981). *Acta Cryst.* **A37**, 734–741.
- SHANNON, R. D. & PREWITT, C. T. (1969). *Acta Cryst.* **B25**, 925–946.
- SHELDRIK, G. M. (1976). *SHELX76*. Program for crystal structure determination. Univ. of Cambridge, England.
- SLOBODYANIK, N. S., NAGORNYI, P. G., SKOPENKO, V. V. & LUGOVSKAYA, E. S. (1987). *Russ. J. Inorg. Chem.* **32**(7), 1023–1026.
- SPEER, J. A. & GIBBS, G. V. (1976). *Am. Mineral.* **61**, 238–247.
- STUCKY, G. D., PHILLIPS, M. L. F. & GIER, T. E. (1989). *Chem. Mater.* **1**(5), 492–509.
- TORDJMAN, I., MASSE, R. & GUITEL, J. C. (1974). *Z. Kristallogr.* **139**, 103–115.
- WATKIN, D. J., CARRUTHERS, J. R. & BETTERIDGE, P. W. (1985). *CRYSTALS User Guide*. Chemical Crystallography Department, Univ. of Oxford, England.
- YANOVSKII, V. K. & VORONKOVA, V. I. (1980). *Phys. Status Solidi a*, **93**, 665–668.
- ZUMSTEG, F. C., BIERLEIN, J. D. & GIER, T. E. (1976). *J. Appl. Phys.* **47**(11), 4980–4985.

Acta Cryst. (1990). **B46**, 343–347

Electron Density Distribution in Crystals of Sodium Nitrite at 120 K

BY MASAMI OKUDA, SHIGERU OHBA AND YOSHIHIKO SAITO*

Department of Chemistry, Faculty of Science and Technology, Keio University, Hiyoshi 3, Kohoku-ku, Yokohama 223, Japan

TETSUZO ITO

Department of Chemical Technology, Kanagawa Institute of Technology, Atsugi 243–02, Japan

AND IWAO SHIBUYA

Research Reactor Institute, Kyoto University, Kumatori, Sennan-gun, Osaka 590–04, Japan

(Received 16 January 1990; accepted 25 January 1990)

Abstract

The electron density distribution in crystals of ferroelectric sodium nitrite has been determined on the basis of the intensity data collected at 120 K. NaNO_2 , $M_r = 69.0$, orthorhombic, $Im2m$, $a = 3.518$ (1), $b = 5.535$ (1), $c = 5.382$ (1) Å, $V = 104.8$ (1) Å³, $Z = 2$, $\text{Mo } K\alpha_1$, $\lambda = 0.7093$ Å, $\mu = 0.365$ mm⁻¹, $F(000) = 68$, final $R = 0.013$ for 437 observed unique reflections after the multipole refinement. The N—O bonding electron and the lone-pair electrons of N and O atoms corresponding to sp^2 hybridization are clearly observed. The effective charges for N and O atoms were estimated to be -0.18 (10) and -0.41 (5) e, respectively. The results are compared with those for $\text{LiNO}_2 \cdot \text{H}_2\text{O}$.

Introduction

Sodium nitrite is one of the well known ferroelectrics and extensive studies have been reported on the crystal structure at various temperatures (Ziegler, 1931; Strijk & MacGillavry, 1943; Kay & Frazer, 1961; Kay, 1972; Kay, Gonzalo & Maglic, 1975). In the present study the charge distribution in the NO_2^-

ion has been examined, which may be indispensable in estimating the lattice energy of the structure. In the calculation of the deformation density for the non-centrosymmetric structure, the spherical independent atom model (IAM) imposes a significant bias on the phase angle of the structure factor. This inadequacy should be removed by the aspherical-atom model (Hirshfeld, 1971; Harel & Hirshfeld, 1975; Ito & Shibuya, 1977). The present study adopted the multipole expansion method, and examined the negligibility of high-order multipoles. The necessity of this examination was discussed by Hansen (1988). To compare with the centrosymmetric case, the same investigation was made for $\text{LiNO}_2 \cdot \text{H}_2\text{O}$, for which X-ray intensity data collected at 120 K were available (Ohba, Kikkawa & Saito, 1985). The determination of the theoretical deformation density by an *ab initio* molecular-orbital calculation has been reported previously (Kikkawa, Ohba, Saito, Kamata & Iwata, 1987).

Experimental

Colorless prismatic crystals of NaNO_2 were grown from aqueous solution. A part of the hard crystal was ground by an Enraf–Nonius spherizer in a dry

* To whom correspondence should be addressed.

N_2 atmosphere. A spherical crystal of diameter 0.35 (1) mm was mounted on a Rigaku AFC-5 four-circle diffractometer with graphite-monochromated $Mo K\alpha_1$ radiation and maintained at 120 K in a stream of cold N_2 gas. Peak half width of the rocking curve of low-order reflections was 0.28° , suggesting large mosaicity caused by grinding. However, it was advantageous in this case to prevent the severe extinction effect of as-grown crystals. X-ray intensity measurement was performed up to $2\theta = 120^\circ$ ($h - 8 \rightarrow 8$, $k - 13 \rightarrow 13$, $l 0 \rightarrow 13$) by ω scan technique with scan speed 6° min^{-1} in θ and scan width 3.5° . For the high-angle region with $100 < 2\theta < 120^\circ$ ($h - 8 \rightarrow 8$, $k - 13 \rightarrow 13$, $l 0 \rightarrow 13$), a θ - 2θ scan was also performed in order to cover the $K\alpha_1$ - $K\alpha_2$ splitting and the $|F_o|$ value was used in the refinement if it was greater than that of the ω scan. The same procedure proved to be effective for iron metal (Ohba, Saito & Noda, 1982). Five standard reflections showed no variation. Cell parameters were refined by least squares for 21 2θ values ($60 < 2\theta < 90^\circ$). 1685 reflections were measured; 1474 reflections observed with $|F_o| > 3\sigma(|F_o|)$, 437 unique reflections assuming mmm point symmetry. The real point group is $m2m$ and the b axis is a polar direction. However, the absolute polarity cannot be determined because of the domain structure of the ferroelectric crystal. In the present study Friedel's rule was assumed to hold and the imaginary part of the anomalous scattering was neglected. A reasonable internal agreement factor, $R_{\text{int}} = 0.016$, was obtained with this approximation. Correction for absorption was made ($\mu r = 0.064$, $0.909 < A < 0.910$). Conventional refinement was at first performed by the full-matrix least-squares program *RADIEL* (Coppens, Guru Row, Leung, Stevens, Becker & Yang, 1979). Reported atomic coordinates (Kay & Frazer, 1961) were utilized as starting parameters. The function $\sum w(|F_o| - |F_c|)^2$ was minimized with weight $w^{-1} = \sigma^2(|F_o|) + (0.015|F_o|)^2$. Positional and thermal parameters were determined based on high-order reflections with $\sin\theta/\lambda \geq 0.7 \text{ \AA}^{-1}$. An isotropic secondary-extinction correction parameter (Becker & Coppens, 1975) did not reduce the R factor significantly. At this stage of the refinement, $R = 0.019$, $wR = 0.025$, $S = 1.2$ for 437 unique reflections, reflection/parameter = 31.2, $\Delta/\sigma < 0.004$. Atomic scattering factors and the real part of the anomalous scattering were taken from *International Tables for X-ray Crystallography* (1974). Calculations were carried out on a FACOM M-380R computer of Keio University. Multipole refinements were then carried out with the program *MOLLY* (Hansen & Coppens, 1978). Multipoles were included up to hexadecapole. The number of multipole parameters for N and O atoms is nine and fifteen, respectively. The radial functions were $r^{n(l)}\exp(-\zeta r)$ with $n(l) = 2, 2, 3$ and 4 (for $l = 1, 2, 3$

and 4, respectively). An extinction parameter was not introduced. The core and valence scattering factors of N and O atoms and the scattering factors of the Na^+ ion were taken from *International Tables for X-ray Crystallography* (1974). The charge of the unit cell was constrained to be neutral with a fixed single positive charge of Na^+ . Multipole, radial (κ) and shielding (ζ) parameters were refined based on all the reflections. Final $R = 0.013$, $wR = 0.019$ and $S = 0.9$ for 437 unique reflections, $\kappa(N) = 0.98$ (1), $\kappa(O) = 0.98$ (1), $\zeta(N) = 3.7$ (2), $\zeta(O) = 3.7$ (3) \AA^{-1} , $\Delta/\sigma < 0.2$, reflection/parameter = 15.1. Atomic coordinates and anisotropic thermal parameters are listed in Table 1.* Multipole refinement for $LiNO_2 \cdot H_2O$ was also carried out in a similar manner using the X-ray data at 120 K (Ohba, Kikkawa & Saito, 1985). The charge of the water molecule was constrained to be zero. Final $R = 0.019$, $wR = 0.023$ and $S = 1.2$ for 1512 observed unique reflections, $\Delta/\sigma < 0.02$, reflection/parameter = 12.9. By introducing the charge asphericity into the model structure the R values reduced significantly: $0.019 \rightarrow 0.013$ for $NaNO_2$, and $0.028 \rightarrow 0.019$ for $LiNO_2 \cdot H_2O$.

Discussion

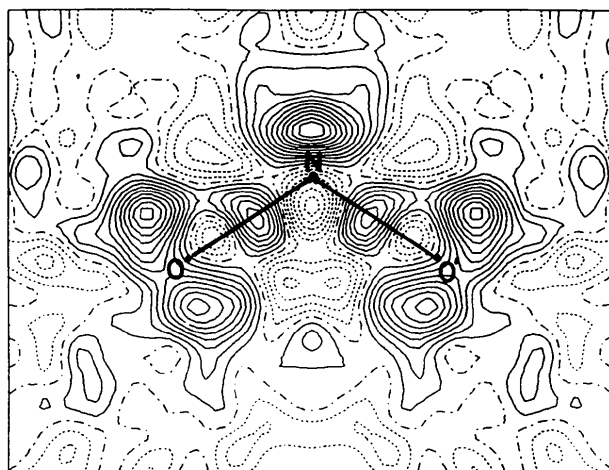
The N—O bond distance and O—N—O bond angle in NO_2^- are $1.2547(6) \text{ \AA}$ and $114.63(2)^\circ$. Fig. 1 shows the deformation density (a) on the NO_2 plane and (b) perpendicular to it containing the N—O axis in $NaNO_2$ after multipole refinement. The features corresponding to sp^2 hybridization of N and O atoms are remarkable. For comparison, the difference density before phase improvement is shown in Fig. 2. The phase improvement by the aspherical-atom model is obvious. To check the sufficiency of the multipole terms, a tentative refinement was performed neglecting hexadecapoles. In Fig. 3 the model deformation densities including (a) up to octapole ($l \leq 3$) and (b) up to hexadecapole ($l \leq 4$), are compared. The features in the experimental deformation map are almost reproduced at the octapole level. The height of the N—O bonding peak and the form of the lone-pair peaks in the model deformation map were improved by adding hexadecapoles. Terms higher than hexadecapole seemed to be negligible. The same conclusion was obtained for $LiNO_2 \cdot H_2O$ crystals, which are centrosymmetric (see Fig. 4). The aspherical-atom model using up to hexadecapoles succeeded quite well in reproducing deformation density.

* Lists of structure factors of $NaNO_2$ have been deposited with the British Library Document Supply Centre as Supplementary Publication No. SUP 52710 (5 pp.). Copies may be obtained through The Technical Editor, International Union of Crystallography, 5 Abbey Square, Chester CH1 2HU, England.

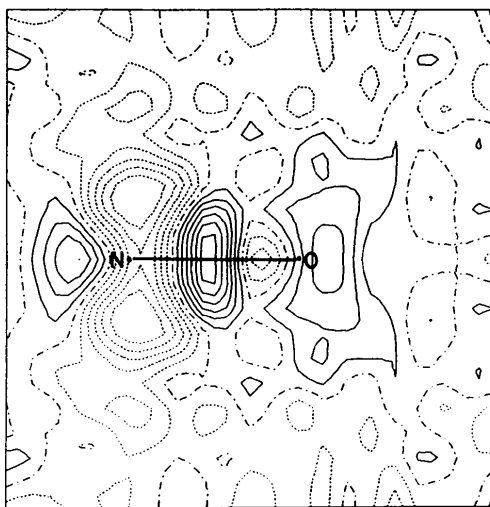
Table 1. *Positional parameters* ($\times 10^5$) and *anisotropic thermal parameters* ($\text{\AA}^2 \times 10^4$)

U_{11} , ... and U_{23} are defined as: $\exp[-2\pi^2(h^2a^{*2}U_{11} + \dots + 2hka^*b^*U_{12} + \dots)]$ where a^* 's, b^* 's and c^* 's are the reciprocal lattice constants.

	<i>x</i>	<i>y</i>	<i>z</i>	<i>B</i> / <i>B</i> _{eq} ($\text{\AA}^2 \times 10$)		
Na	0	58814 (10)	0	8 (1)		
O	0	0	19620 (8)	10 (1)		
N	0	12244 (13)	0	9 (1)		
	U_{11}	U_{22}	U_{33}	U_{12}	U_{13}	U_{23}
Na	124 (1)	99 (1)	99 (1)	0	0	0
O	165 (1)	125 (1)	86 (1)	0	0	13 (1)
N	148 (2)	89 (2)	90 (2)	0	0	0



(a)



(b)

Fig. 1. Observed multipole deformation density, $\Delta\rho_{\text{def}} = \rho_{\text{obs, multipole}} - \rho_{\text{calc, spherical}}$, (a) on the NO_2 plane and (b) on the plane containing the N—O bond axis and perpendicular to the NO_2 plane in NaNO_2 at 120 K after the multipole refinement. Contour intervals at 0.05 e \AA^{-3} . Negative contours are broken, zero contours chain-dotted. The standard deviation is 0.11 e \AA^{-3} in the general position.

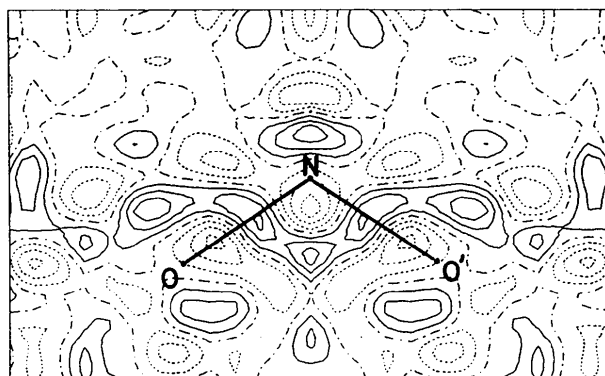
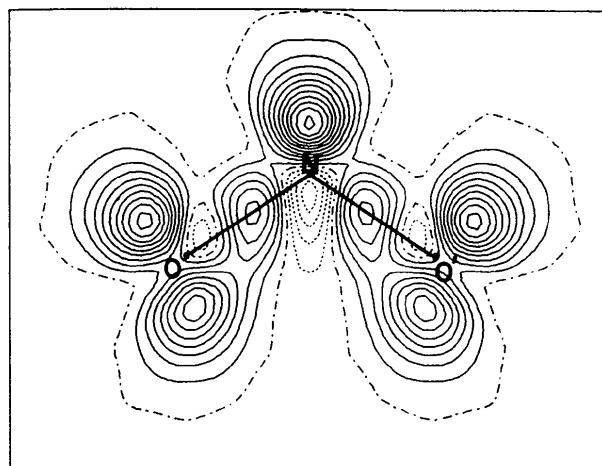
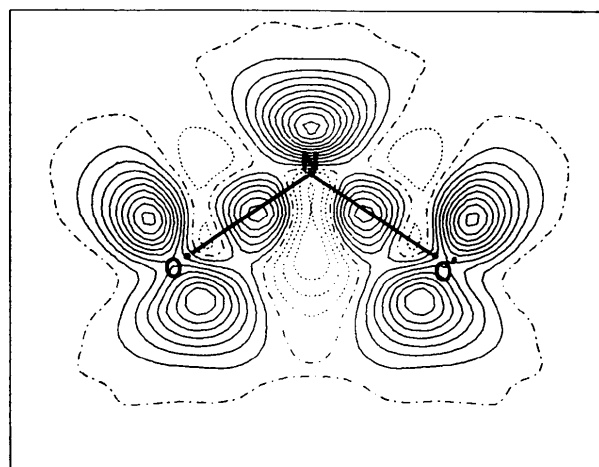


Fig. 2. Observed deformation density on the NO_2 plane in NaNO_2 before the phase improvement. Contour intervals at 0.05 e \AA^{-3} .

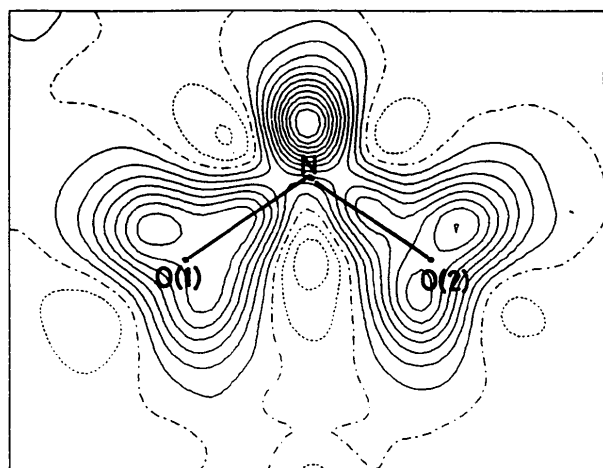


(a)

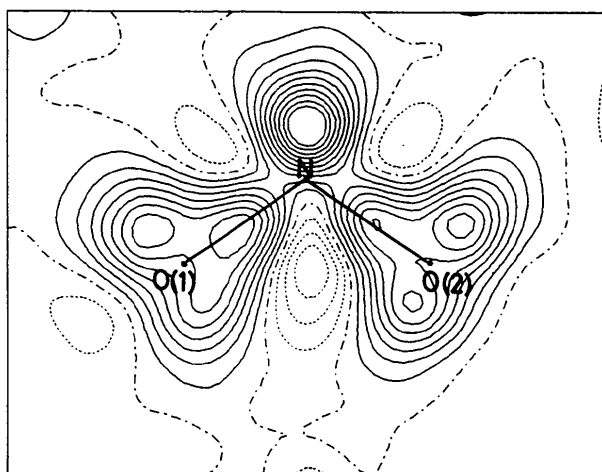


(b)

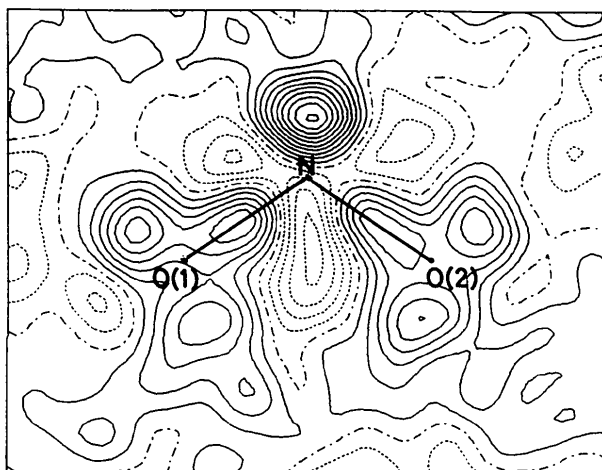
Fig. 3. Model deformation density, $\Delta\rho_{\text{model}} = \rho_{\text{calc, multipole}} - \rho_{\text{calc, spherical}}$, on the NO_2 plane of NaNO_2 including (a) up to octapole terms ($l \leq 3$) and (b) up to hexadecapole terms ($l \leq 4$). Contour intervals at 0.05 e \AA^{-3} .



(a)



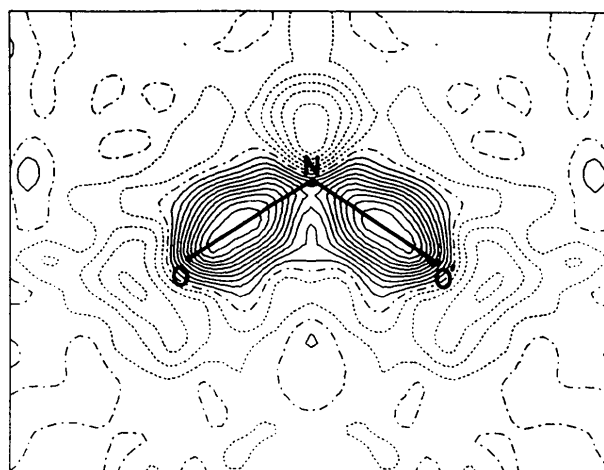
(b)



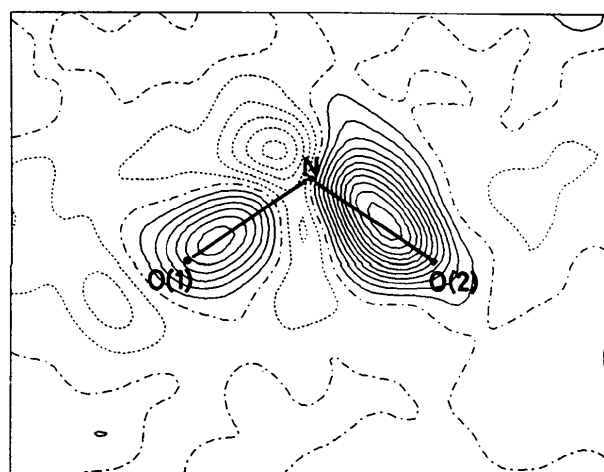
(c)

Fig. 4. Model deformation density on the NO_2 plane of $\text{LiNO}_2 \cdot \text{H}_2\text{O}$ including (a) up to octapole terms ($l \leq 3$) and (b) up to hexadecapole terms ($l \leq 4$). (c) Observed multipole deformation map of the NO_2 plane in $\text{LiNO}_2 \cdot \text{H}_2\text{O}$. Contour intervals at $0.05 \text{ e } \text{Å}^{-3}$.

Fig. 5 shows the observed multipole deformation density with reference to the oriented-atom model (OAM), which was proposed by Schwarz, Valtazanos & Ruedenberg (1985) to remove the effects of hybridization and different occupation of electrons in atomic orbitals from the deformation density. In this case sp^2 hybridization was assumed for neutral N and O atoms with the electron configurations of $(h_1)^2(h_2)^1(h_3)^1(\pi)^1$ for N and $(h_1)^1(h_2)^2(h_3)^2(\pi)^1$ for O atoms (for notation of the atomic orbitals see Fig. 6). The OAM was constructed with multipole functions as described before (Takazawa, Ohba & Saito, 1989). With reference to OAM the electron accumulation on the N—O bond axis can be seen remarkably. The effective charges of the N and O atoms are -0.18 (10) and -0.41 (5) e respectively for NaNO_2 and $+0.09$ (5) and -0.55 (4) e for $\text{LiNO}_2 \cdot \text{H}_2\text{O}$. The electron



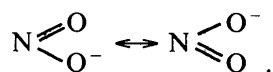
(a)



(b)

Fig. 5. Observed deformation density based on OAM (a) in NaNO_2 and (b) in $\text{LiNO}_2 \cdot \text{H}_2\text{O}$. Contour intervals at $0.10 \text{ e } \text{Å}^{-3}$.

occupancies in valence orbitals for the N and O atoms in sp^2 hybridization, deduced from the refined multipole coefficients, are shown in Fig. 6. The simultaneous equations for the occupancies of the valence orbitals and the multipole coefficients were solved by the least-squares method. The electron occupancies in σ -bonding orbitals of the N and O atoms are more than one [1.33 (2) and 1.41 (8) in NaNO_2], suggesting electron accumulation on the N—O bond axis. The deficiency in electron population of the π orbital of N can be seen in Fig. 1(b). The estimated populations of the π orbitals are 0.91 (6)–0.97 (3) and 1.36 (18)–1.52 (8) for N and O atoms, respectively. The theoretical values are 0.95 and 1.34 from Mulliken population analysis (Kikkawa, Ohba, Saito, Kamata & Iwata, 1987). This accords with the conjugation concept,



The negative charge of the NO_2^- ion is almost localized at the terminal O atoms, which have lone-pair orbitals in the molecular plane. This is the reason why the metal cations preferentially occupy the bridged position between the two O atoms of an NO_2^- ion in the crystals of nitrite salts (Aoyama, Ohba & Saito, 1988). The coloration of nitrite salts

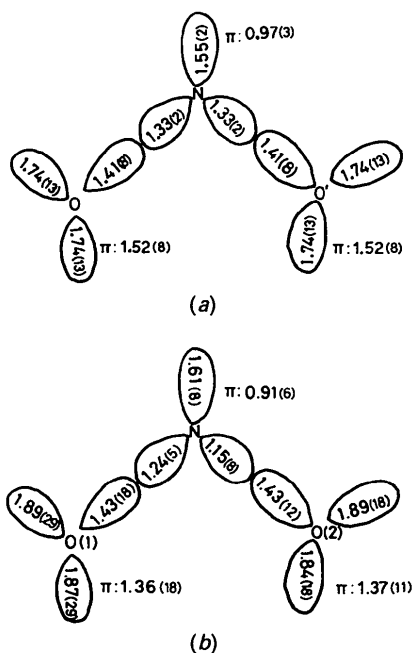


Fig. 6. The occupancies of the valence orbitals for the N and O atoms (a) in NaNO_2 and (b) in $\text{LiNO}_2 \cdot \text{H}_2\text{O}$.

of certain post-transition metal cations having relatively large electronic affinity can be explained in terms of partial allowance for the spin-forbidden $T_1(n\pi^*) \leftarrow S_0$ transition of the NO_2^- ion as a result of perturbation through the metal—O interactions (McGlynn, Azumi & Kumar, 1981). The highest occupied non-bonding molecular orbital of the NO_2^- ion is constructed predominantly with the oxygen $2p$ orbitals parallel to the twofold axis of the ion. Especially in the silver salts AgNO_2 (Ohba & Saito, 1981) and $\text{Ag}_2\text{Li}(\text{NO}_2)_3$ (Ohba, Matsumoto, Ishihara & Saito, 1986), short Ag—N distances can be seen besides the Ag—O bonds. However, the temperature dependence of the disorder of nitrite ions in $\text{AgNa}(\text{NO}_2)_2$ suggests that the Ag—O bond is stronger than the Ag—N bond (Ishihara, Ohba, Saito & Shiozaki, 1987). There is no doubt that the main interaction in NaNO_2 is the attraction between the Na and O atoms.

References

- AOYAMA, T., OHBA, S. & SAITO, Y. (1988). *Acta Cryst.* **C44**, 1703–1707.
- BECKER, P. J. & COPPENS, P. (1975). *Acta Cryst.* **A31**, 417–425.
- COPPENS, P., GURU ROW, T. N., LEUNG, P., STEVENS, E. D., BECKER, P. J. & YANG, Y. W. (1979). *Acta Cryst.* **A35**, 63–72.
- HANSEN, N. K. (1988). *Acta Cryst.* **A44**, 1097.
- HANSEN, N. K. & COPPENS, P. (1978). *Acta Cryst.* **A34**, 909–921.
- HAREL, M. & HIRSHFELD, F. L. (1975). *Acta Cryst.* **B31**, 162–172.
- HIRSHFELD, F. L. (1971). *Acta Cryst.* **B27**, 769–781.
- International Tables for X-ray Crystallography* (1974). Vol. IV. Birmingham: Kynoch Press. (Present distributor, Kluwer Academic Publishers, Dordrecht.)
- ISHIHARA, M., OHBA, S., SAITO, Y. & SHIOZAKI, Y. (1987). *Acta Cryst.* **B43**, 160–164.
- ITO, T. & SHIBUYA, I. (1977). *Acta Cryst.* **A33**, 71–74.
- KAY, M. I. (1972). *Ferroelectrics*, **4**, 235–243.
- KAY, M. I. & FRAZER, B. C. (1961). *Acta Cryst.* **14**, 56–57.
- KAY, M. I., GONZALO, J. A. & MAGLIC, R. (1975). *Ferroelectrics*, **9**, 179–186.
- KIKKAWA, T., OHBA, S., SAITO, Y., KAMATA, S. & IWATA, S. (1987). *Acta Cryst.* **B43**, 83–85.
- MCGLYNN, S. P., AZUMI, T. & KUMAR, D. (1981). *Chem. Rev.* **81**, 475–489.
- OHBA, S., KIKKAWA, T. & SAITO, Y. (1985). *Acta Cryst.* **C41**, 10–13.
- OHBA, S., MATSUMOTO, F., ISHIHARA, M. & SAITO, Y. (1986). *Acta Cryst.* **C42**, 1–4.
- OHBA, S. & SAITO, Y. (1981). *Acta Cryst.* **B37**, 1911–1913.
- OHBA, S., SAITO, Y. & NODA, Y. (1982). *Acta Cryst.* **A38**, 725–729.
- SCHWARZ, W. H. E., VALTANOS, P. & RUEDEBERG, K. (1985). *Theor. Chim. Acta*, **68**, 471–506.
- STRIJK, B. & MACGILLAVRY, C. H. (1943). *Recl Trav. Chim. Pays-Bays*, **62**, 705–712.
- TAKAZAWA, H., OHBA, S. & SAITO, Y. (1989). *Acta Cryst.* **B45**, 432–437.
- ZIEGLER, G. E. (1931). *Phys. Rev.* **38**, 1040–1047.